An improved comprehensive learning: particle swarm optimization: extended Kalman filtering method for the online high-precision state of charge and model parameter co-estimation of lithium-ion batteries.

SHEN, X., WANG, S., YU, C., QI, C., LI, Z. and FERNANDEZ, C.

2023

An Improved Comprehensive Learning - Particle Swarm Optimization - Extended Kalman Filtering Method for the Online High-Precision State of Charge and Model Parameter Co-Estimation of Lithium-Ion Batteries

Journal:	*Journal of The Electrochemical Society*
Manuscript ID	JES-110146.R1
Manuscript Type:	Research Paper
Date Submitted by the Author:	10-Jun-2023
Complete List of Authors:	shen, xianfeng; Southwest University of Science and Technology, Wang, Shunli; Southwest University of Science and Technology Yu, Chun-Mei; Southwest University of Science and Technology, School of Information Engineering qi, chuangshi; Southwest University of Science and Technology Li, Zehao; Southwest University of Science and Technology Fernandez, Carlos; Robert Gordon University
Keywords:	Lithium-ion batteries, Second-order RC model, comprehensive learning particle swarm optimization, State of charge, extended Kalman filter algorithm

An Improved Comprehensive Learning - Particle Swarm Optimization - Extended Kalman Filtering Method for the Online High-Precision State of Charge and Model Parameter Co-Estimation of Lithium-Ion Batteries

Xianfeng Shen,[1] Shunli Wang,[1,2,z] Chunmei Yu,[1] Chuangshi Qi,[1] Zehao Li,[1] Carlos Fernandez[3]

[1]School of Information Engineering, Southwest University of Science and Technology, Mianyang 621010, China

[2]School of Electrical Engineering, Sichuan University, Chengdu 610065, China

[3]School of Pharmacy and Life Sciences, Robert Gordon University, Aberdeen, United Kingdom

Abstract

The precise assessment of the state of charge (SOC) of lithium-ion batteries (LIBs) is critical in battery management systems. This work offers a comprehensive learning particle swarm optimization (CLPSO) and extended Kalman filter (EKF) technique to forecast the SOC of LIBs in order to obtain an accurate SOC estimate for power batteries. Firstly, to address the challenge of identifying various parameters of the battery model, the bilinear transformation technique is employed to determine the parameters of the second-order RC equivalent circuit model. Secondly, to improve the fitness values for the conventional PSO algorithm, which is prone to entering local optimality, a learning strategy (f_i) is added to the particle velocity update method. The optimized PSO and EKF algorithms are integrated to perform online prediction of the SOC of LIBs. The experimental results demonstrate that under the conditions of the Beijing Bus Dynamic Stress Test (BBDST), Dynamic Stress Test (DST), and Hybrid Pulse Power Characterization Test (HPPC), the parameter identification inaccuracy of CLPSO is restricted to 1%. After multi-metric evaluation, the maximum error and mean absolute error of the CLPSO-EKF algorithm in SOC estimation are 0.32% and 0.0652%, respectively, demonstrating a higher robustness and accuracy advantage over other versions.

1 Introduction

Due to their high energy density, extended lifespan, and low self-discharge rate, LIBs are frequently utilized in electric cars. One of the major technologies for electric vehicle battery management, which is crucial for battery protection, lifetime prediction, and temperature control, is the battery SOC estimate [1–3]. Therefore, correct SOC estimate is crucial for both theoretical studies and real-world battery applications [4–6].

The ampere-time integration approach is one of the current typical algorithms for power battery charge state SOC estimation [7] open-circuit voltage method [8,9], neural network method [10,11], and EKF method [12]. Each of these has flaws, and the algorithm's accuracy needs to be increased. Although simpler than the ampere-time integration method, it can be affected by the initial state of SOC [13,14]. The relevant state of the power cell is determined by the open-circuit voltage method, which is based on the SOC-OCV relationship curve. This method is not

appropriate for online estimation of SOC because it requires that the power cell is in an open-circuit state and stationary for a sufficient amount of time [15–17]. To achieve high accuracy, the neural network-based method for SOC estimate needs to be trained extensively on the data over a long period [18–20]. Most lithium batteries are estimated in practical life applications using the EKF algorithm, although this algorithm ignores the impact of noise variation on SOC in practical applications [21–23]. Therefore, some scholars proposed to use PSO algorithm to optimize EKF algorithm [24]. However, in the later stage of iterative optimization, the convergence speed of PSO algorithm gradually slowed down, and it was easy to fall into local optimization. In view of the shortcomings of PSO, some scholars proposed a collaborative particle swarm optimization (CPSO) to improve the problems existing in PSO. However, this method is unstable on multiple multi-peak functions, which will eventually lead to errors in the results [25].

There are numerous battery identification techniques, which can be broadly categorized into two groups: the first is based on conventional parameter identification techniques, like least squares [26–28], which is straightforward but produces inaccurate identification results, the method for adaptive fuzzy estimating [29–31], which performs well in nonlinear systems but has significant stability flaws and subpar identification outcomes. Another type of algorithm is based on intelligent optimization, such as genetic algorithms [32–34], however, the calculation is more difficult due to a large amount of data. Although the PSO approach is straightforward to use with several parameters, it has the drawbacks of readily falling into local optimums and poor convergence accuracy [35–37].

Given the above examination, this paper takes the ternary lithium battery as the research object, selects the second-order RC model as the equivalent model of the lithium battery, and the CLPSO as the model parameter identification algorithm, which has certain advantages in terms of reliability and robustness compared with the traditional methods and is simple and easy to implement. Compared with the standard PSO algorithm, it does not have the disadvantages of the PSO algorithm and has higher accuracy. The EKF algorithm is also optimized using the CLPSO algorithm, which uses the historical best information of other particles to update the particle velocity strategy to improve the PSO algorithm. This algorithm avoids falling into prematureness to a certain extent and performs more consistently than the CPSO algorithm on multiple multi-peak functions. The estimated results of SOC were estimated under three complex working conditions: HPPC, BBDST, and DST. Then the convergence, tracking performance, and estimation accuracy under actual working conditions are analyzed.

2 Mathematical Analysis

2.1 Second-order RC modeling

The most common model is the Thevenin model, which can simulate the internal chemical reaction of the battery, but the single RC circuit cannot fully characterize the dynamic characteristics of the lithium battery. The second-order RC model which is based on the Thevenin model,

connects the second-order resistive network in series and uses the resistive circuit's delay properties to replicate the linearity of battery. When compared to the Thevenin model, the simple structure of the second-order RC model and straightforward operation are better able to represent the static and dynamic characteristics of the battery [38,39]. In light of this, parameter identification is performed using the second-order RC model, as demonstrated in Figure 1.

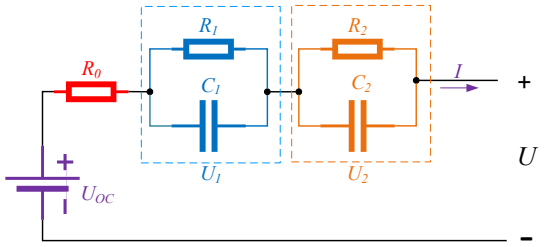

Figure 1. The Second-Order Circuit Model

In Figure 1, U_{OC} is the sign of the open way taken by the electric current electric force, which is related to SOC. R_0 is ohmic inside stopping effect, and R_1 and R_2 denote the battery polarization resistance. C_1 and C_2 denote the battery polarization capacitance, I is the current flowing through the circuit, and U is the terminal voltage of the battery. The voltage and current expressions of the equivalent circuit can be determined using Kirchowski's law by evaluating the created second-order RC model, as shown in equation (1).

$$\begin{cases} U = U_{oc}(soc) - I(t)R_0 - U_1 - U_2 \\ \dfrac{dU_1}{dt} = -\dfrac{U_1}{R_1C_1} + \dfrac{i}{C_1} \\ \dfrac{dU_2}{dt} = -\dfrac{U_2}{R_2C_2} + \dfrac{i}{C_2} \end{cases} \tag{1}$$

For the selected second-order model, $[SOC\ U_1\ U_2]^T$ is selected as the state variable, and the state space equation can be listed as shown in equation (2) by combining equation (1) and the definition of SOC after discretization.

$$\begin{cases} \begin{bmatrix} SOC_{k+1} \\ U_{1,k+1} \\ U_{2,k+1} \end{bmatrix} = \begin{bmatrix} 1 & 0 & 0 \\ 0 & e^{-\Delta t/\tau_1} & 0 \\ 0 & 0 & e^{-\Delta t/\tau_2} \end{bmatrix} \begin{bmatrix} SOC_k \\ U_{1,k} \\ U_{2,k} \end{bmatrix} + \begin{bmatrix} -\dfrac{\eta \Delta t}{Q_N} \\ R_1\left(1 - e^{T/\tau_1}\right) \\ R_2\left(1 - e^{T/\tau_2}\right) \end{bmatrix} I_k + W_k \\ U_{L,k+1} = \begin{bmatrix} \dfrac{\partial U_{OC}}{\partial SOC} & -1 & -1 \end{bmatrix} \begin{bmatrix} SOC_k \\ U_{1,k} \\ U_{2,k} \end{bmatrix} - IR_0 + V_k \end{cases} \tag{2}$$

In the above equation, R_1C_1 and R_2C_2 are the cutoff angular frequencies, Δt is the sampling interval, T is the time constant, $T_1 = R_1C_1$, $T_2 = R_2C_2$, W_k is the state error and V_k is the measurement error, which is the zero-mean white noise of the covariance matrix Q and R, respectively, Q_N is the rated capacity of the battery, η is the Coulomb efficiency, which is set to 0.98. The parameters to be identified by the model are the open-circuit voltage U_{OC} , the ohmic internal resistance R_0, the polarization internal resistance R_1、R_2 and polarization capacitance C_1、C_2.

2.2 CLPSO-based parameter identification

PSO is a population-based optimization tool that is based on the development of the swarm intelligence approach. It is also known as the conventional PSO algorithm [40–42]. The algorithm explores the solution space by following the optimal particle, which is simple to implement and has greater accuracy.

Accepting that the hunt space is D layered, it very well may be communicated as equation (3).

$$\begin{cases} x = \{x_1, x_2, \ldots., x_m\} \\ x_i = \{x_{i1}, x_{i2}, \ldots., x_{iD}\} \\ v_i = \{v_{i1}, v_{i2}, \ldots., v_{iD}\} \\ Pb_i^n = \{Pb_i^1, Pb_i^2, \ldots., Pb_i^n\} \\ Gb_i^n = \{Gb_i^1, Gb_i^2, \ldots., Gb_i^n\} \end{cases} \quad i = 1,2, \ldots., m \tag{3}$$

Where x is the population containing m particles, x_i is the position of the i the particle in D dimensional space for n iterations, indicating a possible position in the search space, also called a candidate solution, v_i is the flight speed of the i the particle in D dimensional space for n iterations, Pb_i^n is the individual extreme value, Gb_i^n is the global extreme value. The particle updates its velocity and position according to the two extreme values, as shown in equation (4) and equation (5).

$$v_i^{n+1} = wv_i^n + a_1b_1(Pb_i^n - x_i^n) + a_2b_2(Gb_i^n - x_i^n) \tag{4}$$

$$x_i^{n+1} = x_i^n + v_i^{n+1} \tag{5}$$

where w is the inertia weight, a_1 and a_2 are two learning factors, which represent the particle state vector and are usually taken as positive integers, b_1 and b_2 are two random numbers between [0,1] and uniformly distributed, n is the number of current iterations.

When the fundamental PSO algorithm is used to identify battery parameters, it is easy to fall into a local optimum during the search for the best. As a result, the best results for parameters like polarization capacitance, polarization resistance, and ohmic resistance are not accurate enough, but these parameters will affect the ability of EKF to estimate the battery SOC, which will result in a significant error in the final estimated SOC. A new learning strategy is proposed based on the classic PSO algorithm, changing the velocity update of the particle equation from (4) to (6) to produce more beneficial results.

$$v_i^{n+1} = wv_i^n + ab_i^n\left(Pb_{fi(n)}^n - x_i^n\right) \tag{6}$$

where $f_i = [f_i(1), f_i(2), \ldots. f_i(n)]$ defines the source of the best experience to be learned by particle i in each dimension, the best experience to be learned by particle i in the nth dimension from the $f(n)$ th particle. For a problem with D dimensions per particle, n dimensions are chosen at random to learn from the population's best experience. The learning probability P_c is then employed in the remaining dimensions to determine whether to learn from the learning paradigm $P_{fi(n)}^n$ at this time, which can be any particle, including the ith particle itself. A random

number will be created for each dimension of particle i, and if this random number is bigger than P_{ci}, the best experience of the particle itself will be learned in that dimension, otherwise, the best experience of other particles will be taught in this dimension. Liang et al [43] postulated that various particles have to vary P_c values, so that the particles in the population have different exploration and exploitation capacities. A random number is created for each dimension of a particle. If P_{ci} is exceeded by this random number, the related dimension will learn from its own best position Pb_i^n, otherwise, it will learn from the best position Pb_i^n of another particle. The following is the equation for the learning probability P_{ci} of particle i is shown as shown in equation (7).

$$P_{ci} = 0.05 + 0.45 \times \frac{exp\left(\frac{5(i-1)}{M-1}\right) - 1}{exp(5) - 1} \tag{7}$$

where the population size is M and the particle number is i.

All Pb_i^n can generate new positions in the search space using the data from the past best placements of various particles. An update threshold m is defined, indicating the maximum number of consecutive failures to get updates that the algorithm will tolerate, to make sure that the particles learn from the paradigm and limit the time wasted going in the wrong direction. A variable called "$flag_i$" is set with a starting value of 0 for each particle i. This variable is used to monitor whether or not the particle has been updated. If the particle's historical best position, Pb_i^n, has changed during the iteration, $flag_i$ is reset to 0, otherwise, $flag_i$ is added to 1. If $flag_i$ reaches the set value of m, it means that the current particle has not been updated for a long time, which means that the template particle it is to learn can no longer guide it to fly to a better solution. At this time, the process in Figure 2 should be followed again, and the particle i should re-select the template to learn.

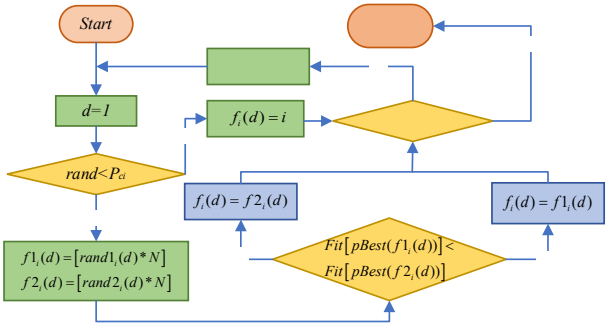

Figure 2. Selection of exemplar dimensions for particle i

The CLPSO algorithm [44–46] has three advantages over the PSO algorithm:

(1) Pb_i^n of all particles could be used as exemplars to direct the flight direction of the particles rather than Pb_i^n and Gb_i^n of particles.

(2) Unlike CLPSO, which allows particles in each dimension to learn the optimal position of various particles in the corresponding dimension, normal PSO requires that all dimensions learn from the same paradigm particles.

(3) While each iteration in the traditional PSO algorithm learns from two paradigms (Pb_i^n and Gb_i^n), particles in the CLPSO algorithm

only learn from one paradigm for each dimension.

The particle Pb_i^n and the particle Gb_i^n belong to the same local optimum region in the CLPSO algorithm's learning strategy, but Pb_i^n can learn from Pb_i^n of other particles to fly in other directions. As a result, the CLPSO algorithm's learning approach can depart from the local optimum thanks to population-wide cooperation. The CLPSO algorithm's progression is depicted in Figure 3.

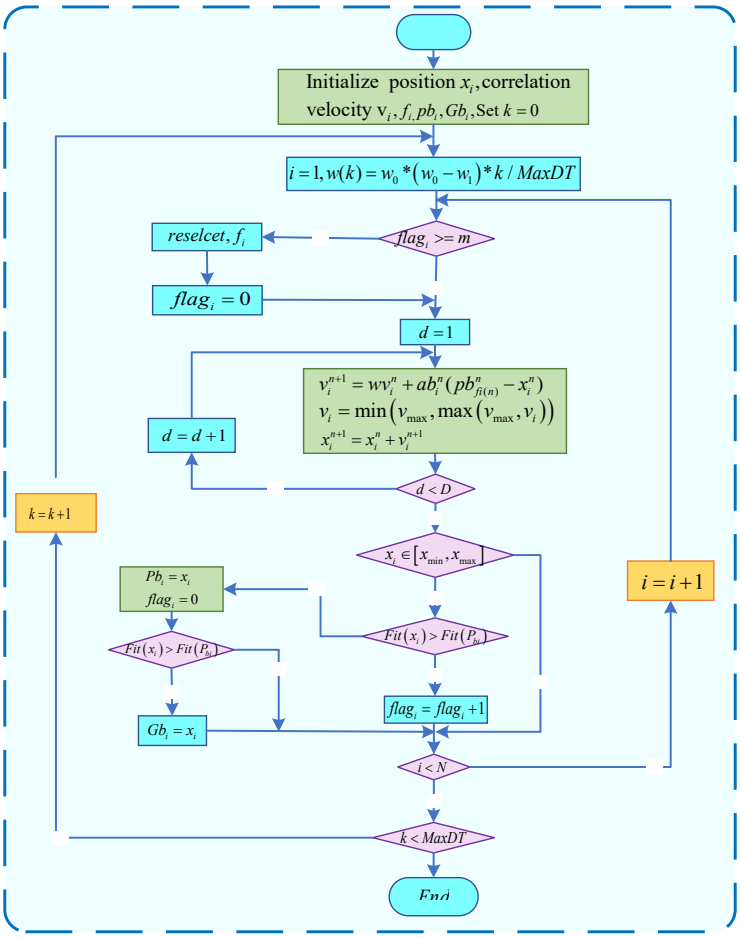

Figure 3. Flow chart of CLPSO algorithm

Analyze excitation response of the battery, gather information on the battery's external input and output of current and voltage, and then indirectly gather data for each parameter in the battery model, using a CLPSO technique. Parameter identification is accomplished by:

Step 1: The objective function will be determined, the speed and position of the group will be initialized, and the overall group size and search space dimension will be determined based on the characteristics of the process. Five battery parameters make up the objective function, and the recursive formula is as shown in equation (8).

$$\begin{cases} U = U_{oc}(SOC) - R_0 I - U_1 - U_2 \\ U_{1,k+1} = U_{1,k} e^{-\Delta t/\tau_1} + R_1 I_k \left(1 - e^{-\Delta t/\tau_1}\right) \\ U_{2,k+1} = U_{2,k} e^{-\Delta t/\tau_2} + R_2 I_k \left(1 - e^{-\Delta t/\tau_2}\right) \end{cases} \tag{8}$$

Step 2: Determine each particle's position and new velocity following equations (4),(5), and (6).

Step 3: Determine the fitness of particles. This paper uses an adaptive variation to reduce the possibility of particles entering the local optimum, preventing the algorithm from entering it. When the cumulative error is used as the fitness function, the following results are shown in equation (9):

$$fitness = \sum_{k=1}^{M} |U_k - U_{mk}| \tag{9}$$

where M denotes the overall number of sampling intervals, U_k denotes the sampling interval, and U_{mk} denotes the sampling interval, denoting the end voltage of the output of the battery model simulation.

Step 4: By contrasting the adaptation value with the best value realized and choosing the optimal value, the objective function is optimized to track the actual voltage.

Step 5: The related parameters also converge to a stable value when the goal function reaches the optimal value, indicating whether this moment has passed or not.

Input voltage and current data, repeated cycles of the aforementioned method, using the aforementioned method to determine the battery identification parameters, obtaining the best results for parameter identification, obtaining a final result by data fitting the identification results, inserting the identification results into the validation model, and then determining the accuracy of this algorithm identification.

2.3 Estimation of battery SOC based on CLPSO-EKF

The EKF method is frequently employed in nonlinear power battery systems. The EKF algorithm's iterative process can be viewed as a Gauss-Newton iterative algorithm, and the algorithm's detailed flow is shown in Figure 4.

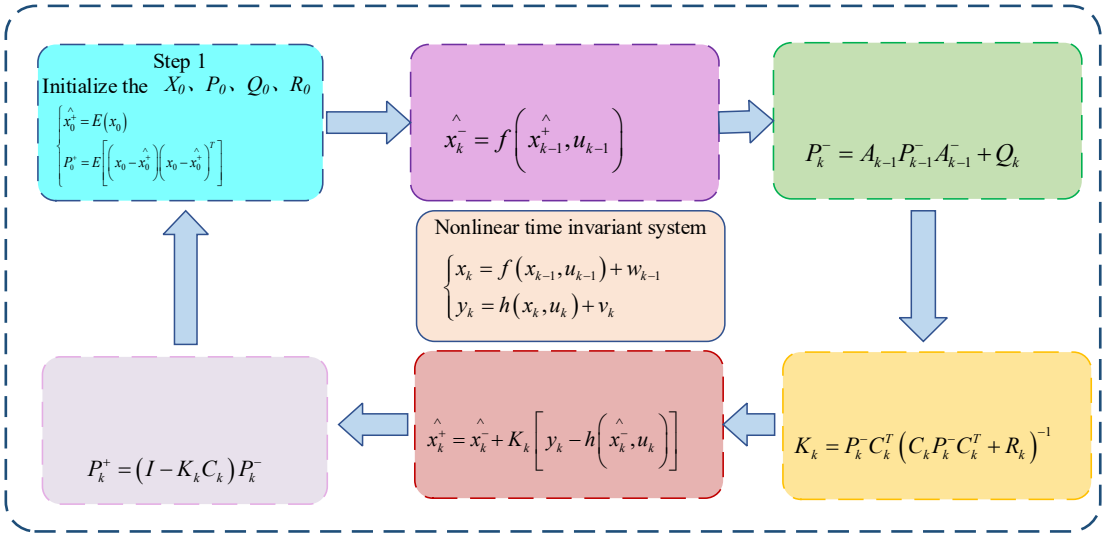

Figure 4. Flowchart of EKF algorithm

By using Taylor's formula to expand the nonlinear system and remove the higher-order terms, the EKF algorithm is utilized to linearize the

nonlinear system. Then the Kalman filter algorithm is used to estimate the SOC. The linearization technique introduces truncation error, even though this is a straightforward method, and it overlooks the impact of noise variation on the SOC. So that the statistical features of the noise in the EKF algorithm can be updated with changes in the estimation results during state estimation, we suggest integrating the CLPSO algorithm into the EKF technique. The fitness function constrains each particle's motion trend as a valid condition to stop the update during the CLPSO-EKF optimization process. The mean square error between the measured value z_k of the EKF transformed second-order RC circuit state equation and the filtered input value x_k is used as the fitness function, and the EKF shall minimize the influence of measurement error and system error in each prediction of the next state process, as shown in equation (17).

$$f(\delta_i^G) = \frac{1}{M}\sum_{k=1}^{M} abs\left(Z_k - X_k(\delta_i^G)\right)^2 \tag{17}$$

In the following formula: M is the number of iterations, δ_i^G is the optimized parameter value of the i the individual at the iteration to the Gth generation. $f(\delta_i^G)$ is the error between the measured value and the input value of the i the individual at the iteration to the G the generation.

Figure 5 depicts the CLPSO-based EKF optimization process, where R represents the measurement noise covariance matrix and Q represents the system noise covariance matrix. By updating the measurement and time depending on the chosen filter parameters, the input value x_k, and the measurement value z_k, the EKF determines the best approximation of the system state at each instant. The CLPSO algorithm is used to optimize the filter R parameters and Q following the values of the objective function and filter parameters at each instant. Up until the optimized state estimates are obtained, the optimized parameters are used as filtering parameters in the EKF.

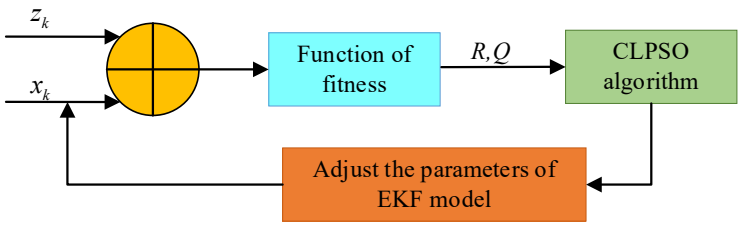

Figure 5. Flowchart of CLPSO-EKF algorithm

The process of CLPSO optimization of the EKF is:

Step 1: Setting the initial values of the state input value x_k and the error covariance matrix z_k of the EKF.

Step 2: Initialize the positions and velocities of all particles in the particle swarm.

Step 3: Set $f(\delta_i^G)$ as the particle i fitness function, and calculate the fitness value.

Step 4: To get the optimum location $P_{fi(n)}^n$ at this time, decide whether the probability P_{ci} is learning to the learning paradigm $P_{fi(n)}^n$ according to the current dimension; if not, resampling is done.

Step 5: The best value is determined by comparing the current value of $f(\delta_i^G)$ with the historical fitness value, if it satisfies the update termination requirement, it is assigned to Gb_i^n in; otherwise, Gb_i^n in remains unchanged.

Step 6: If the update termination condition is satisfied, compare Gb_i^n in to the historical optimal fitness Pb_i^n in of other particles in the swarm, if the value is deemed optimal, Gb_i^n it is assigned to Pb_i^n in; otherwise, Pb_i^n in is left unchanged.

Step 7: Repeat steps (5) and (6) until all particles are compared and the particle value with the optimal solution is output and assigned to the measurement noise covariance matrix R and the system noise covariance matrix Q.

According to the aforementioned analysis, CLPSO-EKF, when compared to EKF, adds the estimation of noise characteristics on the original basis and makes real-time corrections to R and Q to achieve the goal of continuous correction of the SOC estimates of state variables. This resolves issues with the traditional EKF measurement of noise covariance and the impact of SOC valuation bias caused by system noise covariance, thereby increasing the accuracy of SOC estimation.

3 Analysis of experimental results

The effectiveness of the CLPSO algorithm for model parameter identification is therefore verified under BBDST conditions, and SOC experiments are performed under two different complex conditions of HPPC and BBDST and compared with other algorithms. This is done to confirm the scientific validity of the algorithm proposed in this paper.

3.1 Experimental platform construction

LIB with a rated capacity of 72 Ah and a ternary lithium battery with an actual capacity of 69.23 Ah produced by Deliphone Battery Technology Co. The battery test system is BTS200-100-104, provided by Shenzhen Yakeyuan Technology Co. as the charge and discharge test equipment for lithium-ion batteries.A room temperature (25°C) thermostat (TT-5166-7) provides room temperature for the experimental cell.

The experimental platform architecture is shown in Figure 6.

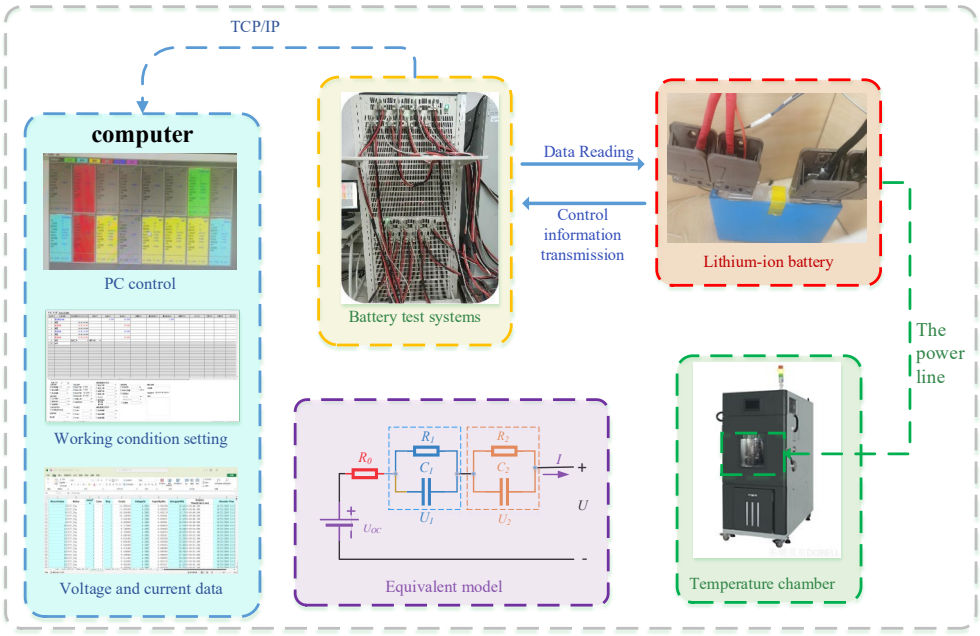

Figure 6. Lithium battery experimental platform architecture

3.2 Results of parameter identification

This paper validates the parameter results under BBDST conditions to obtain the variation of the internal parameters of LIBs at various points and then uses these obtained data as the simulated voltages in the model so that we can compare and analyze the simulated and actual measured voltages, and then we can verify the accuracy of this parameter identification.

The parameters also reach the matching reasonable value when the objective function reaches a steady convergence value. In essence, the objective function search is used to carry out the parameter identification. The CLPSO algorithm is used in this study, C_1 and C_2 are set to 1.3 and 1.7, respectively, w , the inertia weight is set to a maximum of 0.9 and a minimum of 0.4, 50 is the number of populations, and 50 is the maximum number of iterations. The server with a 2.30 GH i7 CPU and 16 G of memory was utilized for computing during the experiment, and the full computation took around 20 seconds. The parameter identification results and the fitness function graph can be obtained by comparing the identified results with the actual values, as shown in Figure 7.

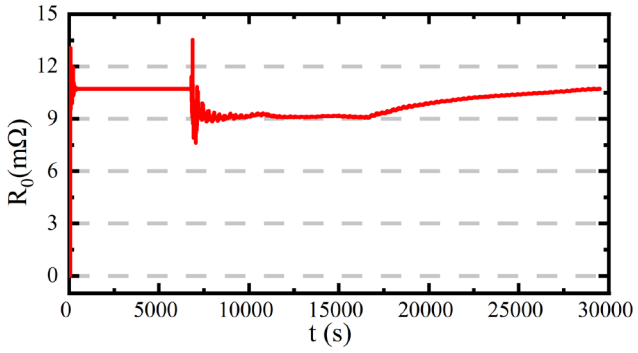

(a) R_0 under parameter identification

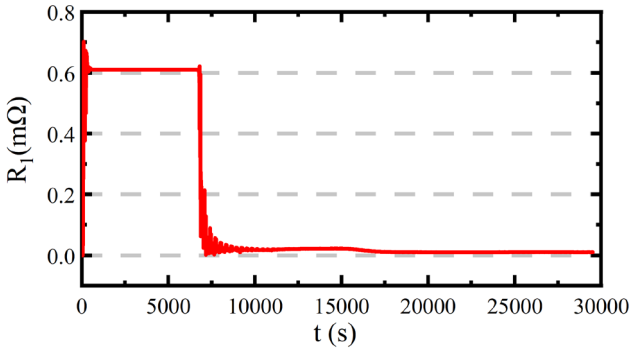

(b) R_1 under parameter identification

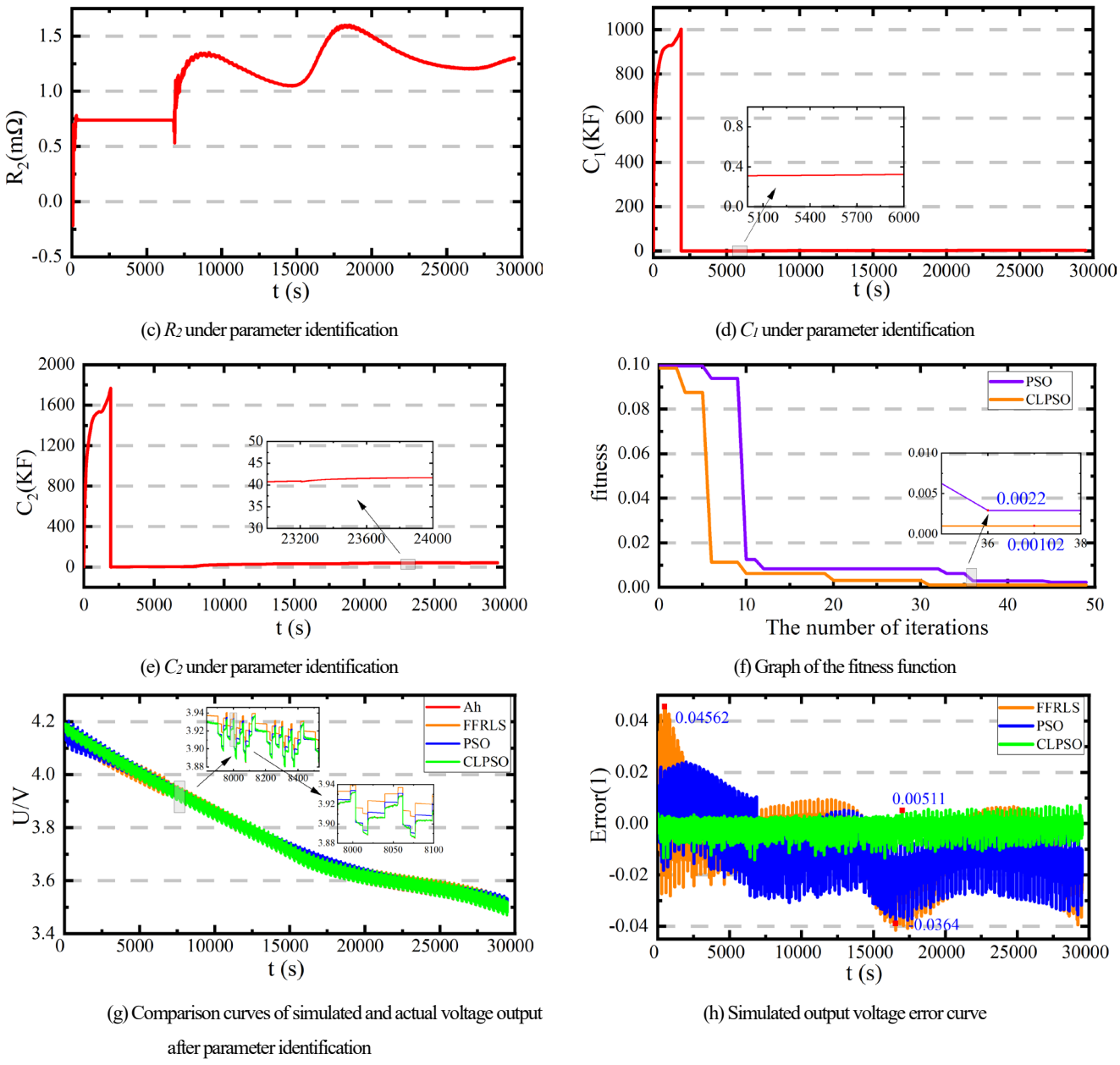

(c) R_2 under parameter identification

(d) C_1 under parameter identification

(e) C_2 under parameter identification

(f) Graph of the fitness function

(g) Comparison curves of simulated and actual voltage output after parameter identification

(h) Simulated output voltage error curve

Figure 7. Parameter identification results and fitness function

Figures 7 (a), (b), (c), (d), and (e) illustrate R_0、R_1、R_2、C_1、C_2 under the identification of the CLPSO algorithm. From the figures, we can see that initially, due to the initial value of each parameter not being set accurately enough, they all fall into the situation of local optimum and fluctuate greatly, but with the continuous iterative update of the algorithm, the parameter values gradually tend to smooth out. When comparing FFRLS, PSO, and CLPSO for parameter identification, it can be observed from Figure 7 (g) that the CLPSO method has a greater impact and a higher level of accuracy. The simulation output voltage error curves between these three different algorithms and the real voltage are shown in Figure 7 (h), and the analysis results show that all three algorithms can identify the battery model parameters with better results. The FFRLS and PSO algorithms are close to one another for the model parameters identification, and the error is within 5%, while the CLPSO algorithm identifies the accuracy within 1%, which is better than the above two algorithms. It is further demonstrated that the CLPSO is quicker and more accurate for

battery model identification by comparing the fitness functions of PSO and CLPSO in Figure 7 (f). The CLPSO algorithm converges with the best fitness value of 0.00102 after 30 iterations, while the standard PSO algorithm converges with the best fitness function value of 0.0022 after 45 iterations. greater accuracy.

3.3 Validation of SOC estimation based on CLPSO-EKF algorithm

The hybrid pulse power characterization (HPPC) operating condition data at room temperature (25°C) is chosen for the model estimate in this research to test the algorithm's precision. Figure 8 (a) compares SOC estimation outcomes for various algorithms using CLPSO parameter identification, while Figure 8 (b) compares estimation errors for various algorithms using the same parameter identification circumstances. These results are then used in the CLPSO-EKF method.

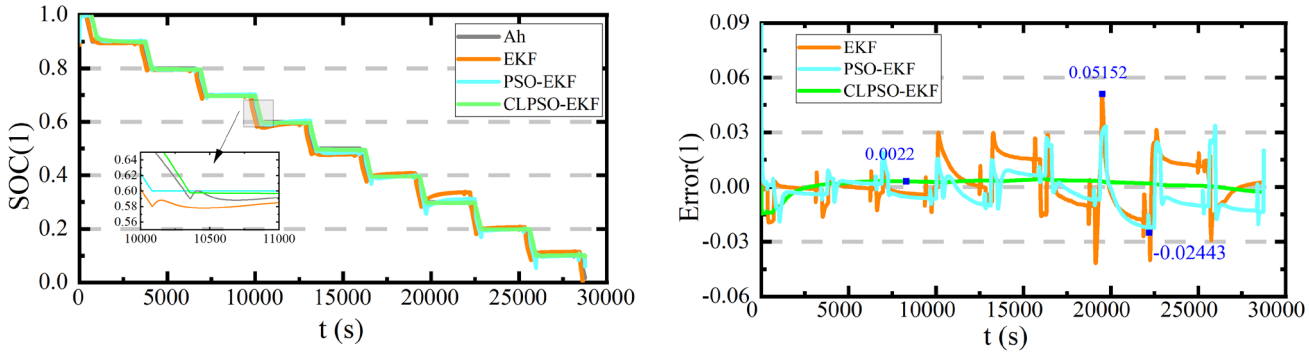

(a) Comparison of SOC estimation results under different algorithms (b) Error of SOC estimation results under different algorithms

Figure 8. SOC estimation results and errors under HPPC working conditions

All three algorithms exhibit a stepped-down tendency over time, as seen in Figure 8 (a). PSO-EKF is superior to the conventional EKF algorithm but also has the drawback of slipping into the local optimum, which is not significant to the optimization of EKF. The estimated value of the EKF method deviates from the reference value. The CLPSO-EKF method produces the best results, while there is a difference from the reference value, it is more stable. Given that the reference value is assumed to be the actual value, the deviation of the CLPSO-departure EKF from the actual value can be viewed as a systematic error and improved by linear compensation. The maximum errors for each of the three algorithms are shown in Figure 8 (b). The maximum errors for the EKF algorithm are 5.152%, and the maximum errors for the PSO-EKF algorithm are 2.443%, demonstrating how the CLPSO-EKF improves the errors brought on by process noise in the pre-discharge period of the EKF and PSO-EKF. And a large convergence is achieved when the CLPSO algorithm is optimized for the EKF method to estimate lithium-ion SOC.

To further validate the estimation algorithm's response to the charge status of the LIB under more complex application situations, the model is simulated and validated using experimental data from the BBDST conditions. The experimental data of BBDST is more convincing in proving the algorithm's viability. Figure 9 (a) compares the SOC estimation results obtained using various algorithms with parameter identification from the CLPSO, and Figure 9 (b) compares the estimation errors obtained using various algorithms with parameter identification from the same source.

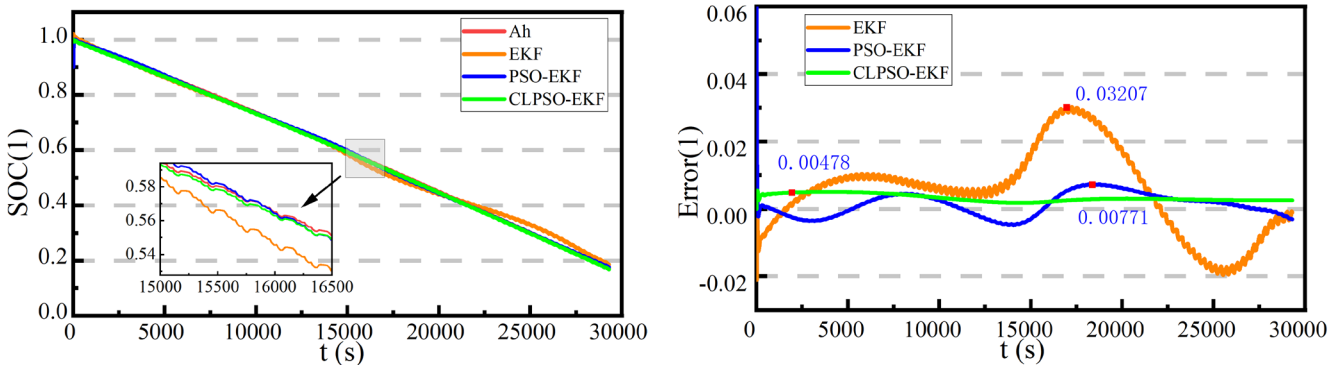

(a) Comparison of SOC estimation results under different algorithms (b) Error of SOC estimation results under different algorithms

Figure 9. SOC estimation results and errors under BBDST working conditions

When comparing the estimation results of the three algorithms in Figure 9, it can be seen that, according to the HPPC condition, all three algorithms converge quickly in the early stage, but as the condition progresses, the estimation error increases. The EKF algorithm deviates significantly in the late stage due to the accumulation of errors, with a maximum error of 3.207%, while the PSO-EKF algorithm optimizes this flaw of the EKF algorithm, but in the early stage. By including learning elements, the CLPSO-EKF reduces its local optimum deficiency. The CLPSO-EKF estimation is the best, and the error bias value always presents a stable state throughout the full experimental process simulation, which is caused by systematic error, and its maximum error is 0.478%. Figure 9 (b) displays the corresponding errors under each of the three techniques. This demonstrates that the CLPSO-EKF algorithm performs significantly better in the estimation of lithium-ion SOC.

The reliability of this algorithm is studied again under the DST condition, which is of greater value for our experimental results analysis. From the error plot in Figure 10, we can see that the error of the EKF algorithm under the DST condition fluctuates greatly, and the EKF algorithm after PSO optimization has improved significantly. The maximum error is reduced from 2.441% to 0.058%, and their maximum error is within 3%, which is within a controllable range. To prevent the PSO algorithm from falling into the local optimum, the CLPSO algorithm is used, and it can be seen from the error plot that the SOC value estimated by the CLPSO-EKF algorithm almost overlaps with the true value, and the error is much lower than that estimated by several other algorithms. This also verifies that the algorithm in this paper is the correct choice of algorithm.

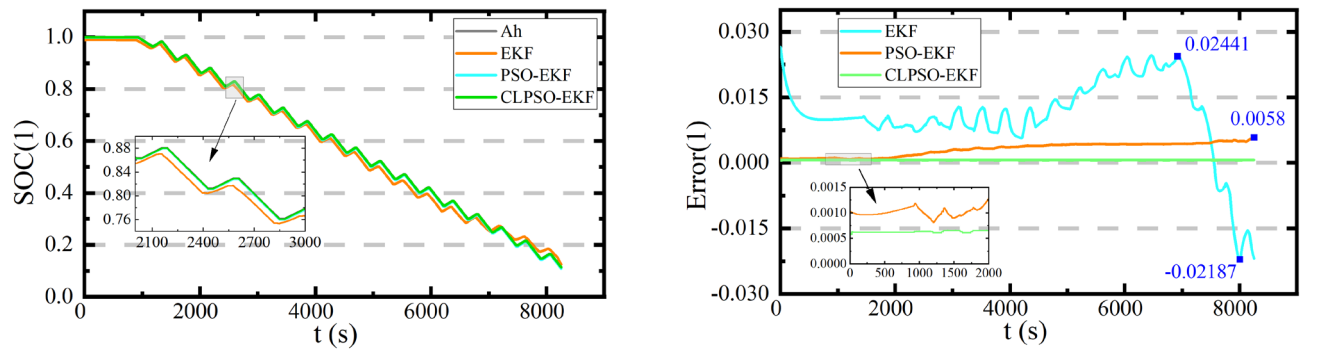

(a) Comparison of SOC estimation results under different algorithms (b) Error of SOC estimation results under different algorithms

Figure 10. SOC estimation results and errors under DST working conditions

According to the research results of the above three working conditions, the CLPSO-EKF algorithm has a high precision effect on SOC estimation. To further confirm the correctness of the proposed algorithm, MAE and RMSE are selected to further compare the calculation results. The detailed calculation as shown in equations (18) and (19).

$$MAE = \frac{\sum_{i=1}^{N} |SOC'(t) - SOC(t)|}{N} \tag{18}$$

$$RMSE = \sqrt{\frac{\sum_{i=1}^{N} \left(SOC'(t) - SOC(t)\right)^2}{N}} \tag{19}$$

The mean absolute error (MAE) represents the mean of the absolute error between the predicted value and the measured value. The smaller the MAE value, the smaller the error between the estimated value and the true value. The root mean square error (RMSE) represents the sample standard deviation (known as the residual) of the difference between the predicted and measured values. RMSE represents the degree of dispersion of the samples. The smaller the RMSE value, the better the prediction ability of the algorithm.

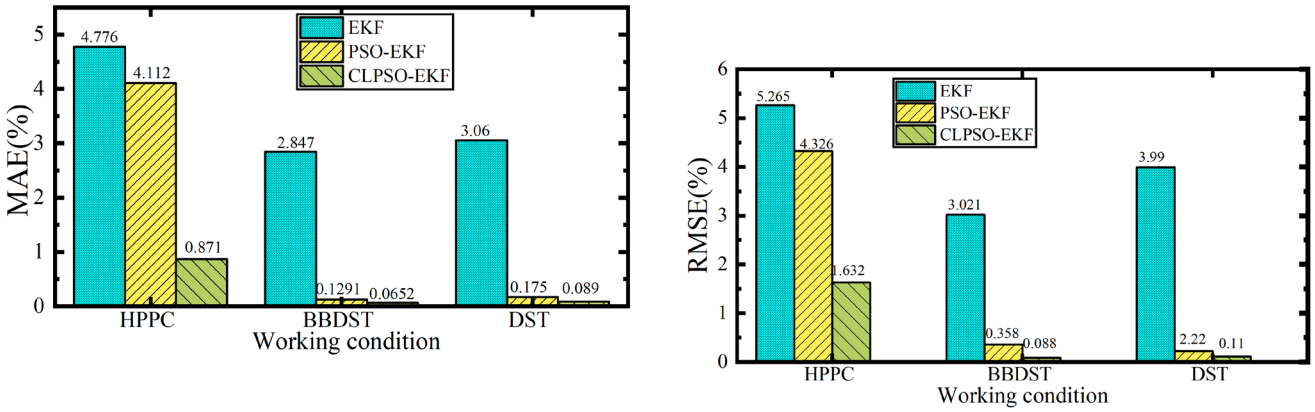

(a) Comparison of MAE estimation results under different working conditions

(b) Comparison of RMSE estimation results under different working conditions

Figure 11. Comparison of error results under different working conditions

The results obtained are shown in Figure 11. It can be seen from the data graph that the error result of CLPSO-EKF is the smallest under three different working conditions. The optimization of the EKF algorithm by CLPSO can accurately estimate SOC with high accuracy and is consistent with the real SOC curve.

4 Conclusion

The major aspect and complexity of LIB state monitoring is accurate SOC estimation. In this paper, we characterize the state and output characteristics of LIBs using a second-order RC model, identify the parameters of the battery model using a CLPSO algorithm, and determine the relationship between the circuit model parameters and the change in LIB charge state at different discharge stages. This clever technique is also utilized to improve the EKF algorithm's accuracy in estimating SOC. The following conclusions are drawn through experimental analysis:

(1) In the parameter identification process, compared to the traditional FFRLS algorithm and PSO algorithm for the problem of multi-parameter identification of battery models, the CLPSO algorithm combined with bilinear transformation processing to identify the parameters of battery models not only achieves the results of online parameter identification but also overcomes the problem that PSO is easy to fall into local optimums. The graph also demonstrates that CLPSO has high accuracy and low error for battery model identification, and the method is easy and not time-consuming, therefore, we can infer that employing the CLPSO algorithm for parameter identification is an innovation in parameter identification.

(2) The learning method (f_i) is used in the battery SOC estimate to optimize several PSO difficulties, such as the tendency to fall into the local optimum and the sluggish convergence speed. Furthermore, the CLPSO algorithm solves the problems of the EKF algorithm in terms of measurement noise covariance and the impact of the SOC valuation bias caused by system noise covariance, and it is known from literature analysis that the CLPSO algorithm is more stable than other improved PSO algorithms. The validation findings show that the error of the CLPSO-EKF estimation of battery SOC is controlled within 0.5% under diverse complex settings, confirming the high accuracy and robustness of the CLPSO-EKF method in LIB SOC estimation.

(3) It is clear from the verification of the entire experimental process in this research that the CLPSO algorithm produces better results, and we can try to apply this strategy to other algorithms more frequently in future work.

Acknowledgments

The work was supported by the National Natural Science Foundation of China (No.62173281,61801407).

References

1. Kulova, T.L.; Fateev, V.N.; Seregina, E.A.; Grigoriev, A.S. A Brief Review of Post-Lithium-Ion Batteries. *Int. J. Electrochem. Sci.* **2020**, *15*, 7242–7259, doi:10.20964/2020.08.22.

2. Yang, J.; Xia, B.; Shang, Y.; Huang, W.; Mi, C.C. Adaptive State-of-Charge Estimation Based on a Split Battery Model for Electric Vehicle Applications. *IEEE Trans. Veh. Technol.* **2017**, *66*, 10889–10898, doi:10.1109/TVT.2017.2728806.

3. Chen, X.-D.; Yang, H.-Y.; Wun, J.-S.; Wang, C.-H.; Li, L.-L. Life Prediction of Lithium-Ion Battery Based on a Hybrid Model. *Energy Exploration & Exploitation* **2020**, *38*, 1854–1878, doi:10.1177/0144598720911724.

4. Xiong, R.; Cao, J.; Yu, Q.; He, H.; Sun, F. Critical Review on the Battery State of Charge Estimation Methods for Electric Vehicles. *IEEE Access* **2018**, *6*, 1832–1843, doi:10.1109/ACCESS.2017.2780258.

5. Fan, B.; Luan, X.; Zhang, R.; Niu, T.; Xie, Y. Research on SOC Estimation Algorithm for Lithium Battery Based on EKF Algorithm and Ampere-Hour Integration Method.; Atlantis Press, December 2017; pp. 101–105.

6. Guo, F.; Hu, G.; Xiang, S.; Zhou, P.; Hong, R.; Xiong, N. A Multi-Scale Parameter Adaptive Method for State of Charge and Parameter Estimation of Lithium-Ion Batteries Using Dual Kalman Filters. *Energy* **2019**, *178*, 79–88, doi:10.1016/j.energy.2019.04.126.

7. Cui, Z.; Wang, L.; Li, Q.; Wang, K. A Comprehensive Review on the State of Charge Estimation for Lithium-Ion Battery Based on Neural Network. *Int. J. Energy Res.* **2022**, *46*, 5423–5440, doi:10.1002/er.7545.

8. Duan, J.; Wang, P.; Ma, W.; Qiu, X.; Tian, X.; Fang, S. State of Charge Estimation of Lithium Battery Based on Improved Correntropy Extended Kalman Filter. *Energies* **2020**, *13*, 4197, doi:10.3390/en13164197.

9. Pang, H.; Wu, L.; Liu, J.; Liu, X.; Liu, K. Physics-Informed Neural Network Approach for Heat Generation Rate Estimation of Lithium-Ion Battery under Various Driving Conditions. *Journal of Energy Chemistry* **2023**, *78*, 1–12, doi:10.1016/j.jechem.2022.11.036.

10. Tang, H.; Wu, Y.; Cai, Y.; Wang, F.; Lin, Z.; Pei, Y. Design of Power Lithium Battery Management System Based on Digital Twin. *J. Energy Storage* **2022**, *47*, 103679, doi:10.1016/j.est.2021.103679.

11. Pang, H.; Geng, Y.; Liu, X.; Wu, L. A Composite State of Charge Estimation for Electric Vehicle Lithium-Ion Batteries Using Back-Propagation Neural Network and Extended Kalman Particle Filter. *J. Electrochem. Soc.* **2022**, *169*, 110516, doi:10.1149/1945-7111/ac9f79.

12. He, D.W.; Zhang, W.; Luo, X.Y. Overview of Power Lithium Battery Modeling and Soc Estimation. *IOP Conf. Ser.: Earth Environ. Sci.* **2020**, *461*, 012032, doi:10.1088/1755-1315/461/1/012032.

13. Tian, J.; Xiong, R.; Shen, W.; Sun, F. Electrode Ageing Estimation and Open Circuit Voltage Reconstruction for Lithium Ion Batteries. *Energy Storage Materials* **2021**, *37*, 283–295, doi:10.1016/j.ensm.2021.02.018.

14. Jibhkate, U.N.; Mujumdar, U.B. Development of Low Complexity Open Circuit Voltage Model for State of Charge Estimation with Novel Curve Modification Technique. *Electrochim. Acta* **2022**, *429*, 140944, doi:10.1016/j.electacta.2022.140944.

15. Zheng, F.; Xing, Y.; Jiang, J.; Sun, B.; Kim, J.; Pecht, M. Influence of Different Open Circuit Voltage Tests on State of Charge Online Estimation for Lithium-Ion Batteries. *Applied Energy* **2016**, *183*, 513–525, doi:10.1016/j.apenergy.2016.09.010.

16. Wang, Q.; Ye, M.; Wei, M.; Lian, G. Optimized Deep Neural Network Enabled Low-Cost State of Charge Estimation for Different Kinds of Lithium-Ion Batteries under Dynamic Load Conditions. *Int. J. Energy Res.*, doi:10.1002/er.8596.

17. Wei, M.; Ye, M.; Li, J.B.; Wang, Q.; Xu, X.X. State of Charge Estimation for Lithium-Ion Batteries Using Dynamic Neural Network Based on Sine Cosine Algorithm. *Proc. Inst. Mech. Eng. Part D-J. Automob. Eng.* **2022**, *236*, 241–252, doi:10.1177/09544070211018038.

18. Chen, J.; Ouyang, Q.; Xu, C.; Su, H. Neural Network-Based State of Charge Observer Design for Lithium-Ion Batteries. *IEEE Trans. Control Syst. Technol.* **2018**, *26*, 313–320, doi:10.1109/TCST.2017.2664726.

19. Zhang, L.; Zhang, L.; Papavassiliou, C.; Liu, S. Intelligent Computing for Extended Kalman Filtering SOC Algorithm of Lithium-Ion Battery. *Wirel. Pers. Commun.* **2018**, *102*, 2063–2076, doi:10.1007/s11277-018-5257-9.

20. Rzepka, B.; Bischof, S.; Blank, T. Implementing an Extended Kalman Filter for SoC Estimation of a Li-Ion Battery with Hysteresis: A Step-by-Step Guide. *Energies* **2021**, *14*, 3733, doi:10.3390/en14133733.

21. Li, W.; Yang, Y.; Wang, D.; Yin, S. The Multi-Innovation Extended Kalman Filter Algorithm for Battery SOC Estimation. *Ionics* **2020**, *26*, 6145–6156, doi:10.1007/s11581-020-03716-0.

22. Zhang, S.; Zhang, X. A Comparative Study of Different Online Model Parameters Identification Methods for Lithium-Ion Battery. *Sci. China Technol. Sci.* **2021**, *64*, 2312–2327, doi:10.1007/s11431-021-1837-0.

23. Du, X.; Meng, J.; Zhang, Y.; Huang, X.; Wang, S.; Liu, P.; Liu, T. An Information Appraisal Procedure: Endows Reliable Online Parameter Identification to Lithium-Ion Battery Model. *IEEE Transactions on Industrial Electronics* **2022**, *69*, 5889–5899, doi:10.1109/TIE.2021.3091920.

24. Yu, X.; Wei, J.; Dong, G.; Chen, Z.; Zhang, C. State-of-Charge Estimation Approach of Lithium-Ion Batteries Using an Improved Extended Kalman Filter. *Energy Procedia* **2019**, *158*, 5097–5102, doi:10.1016/j.egypro.2019.01.691.

25. van den Bergh, F.; Engelbrecht, A.P. A Cooperative Approach to Particle Swarm Optimization. *IEEE Transactions on Evolutionary Computation* **2004**, *8*, 225–239, doi:10.1109/TEVC.2004.826069.

26. Ren, B.; Xie, C.; Sun, X.; Zhang, Q.; Yan, D. Parameter Identification of a Lithium-Ion Battery Based on the Improved Recursive Least Square Algorithm. *IET Power Electronics* **2020**, *13*, 2531–2537, doi:10.1049/iet-pel.2019.1589.

27. Cui, X.; Xu, B. State of Charge Estimation of Lithium-Ion Battery Using Robust Kernel Fuzzy Model and Multi-Innovation UKF Algorithm Under Noise. *IEEE Trans. Ind. Electron.* **2022**, *69*, 11121–11131, doi:10.1109/TIE.2021.3121774.

28. Zand, M.; Nasab, M.A.; Hatami, A.; Kargar, M.; Chamorro, H.R. Using Adaptive Fuzzy Logic for Intelligent Energy Management in Hybrid Vehicles. In Proceedings of the 2020 28th Iranian Conference on Electrical Engineering (ICEE); August 2020; pp. 1–7.

29. Hu, L.; Hu, X.; Che, Y.; Feng, F.; Lin, X.; Zhang, Z. Reliable State of Charge Estimation of Battery Packs Using Fuzzy Adaptive Federated Filtering. *Applied Energy* **2020**, *262*, 114569, doi:10.1016/j.apenergy.2020.114569.

30. Ahmed, R.; Rahimifard, S.; Habibi, S. Offline Parameter Identification and SOC Estimation for New and Aged Electric Vehicles Batteries. In Proceedings of the 2019 IEEE Transportation Electrification Conference and Expo (ITEC); June 2019; pp. 1–6.

31. Ling, L.; Wei, Y. State-of-Charge and State-of-Health Estimation for Lithium-Ion Batteries Based on Dual Fractional-Order Extended Kalman Filter and Online Parameter Identification. *IEEE Access* **2021**, *9*, 47588–47602, doi:10.1109/ACCESS.2021.3068813.

32. Jinlei, S.; Wei, L.; Chuanyu, T.; Tianru, W.; Tao, J.; Yong, T. A Novel Active Equalization Method for Series-Connected Battery Packs Based on Clustering Analysis With Genetic Algorithm. *IEEE Transactions on Power Electronics* **2021**, *36*, 7853–7865, doi:10.1109/TPEL.2021.3049166.

33. Zhang, S.; Zhang, X. A Comparative Study of Different Online Model Parameters Identification Methods for Lithium-Ion Battery. *Sci. China Technol. Sci.* **2021**, *64*, 2312–2327, doi:10.1007/s11431-021-1837-0.

34. Jarrraya, I.; Degaa, L.; Rizoug, N.; Chabchoub, M.H.; Trabelsi, H. Comparison Study between Hybrid Nelder-Mead Particle Swarm Optimization and Open Circuit Voltage-Recursive Least Square for the Battery Parameters Estimation. *J. Energy Storage* **2022**, *50*, 104424, doi:10.1016/j.est.2022.104424.

35. Wang, Z.; Feng, G.; Liu, X.; Gu, F.; Ball, A. A Novel Method of Parameter Identification and State of Charge Estimation for Lithium-Ion Battery Energy Storage System. *J. Energy Storage* **2022**, *49*, 104124, doi:10.1016/j.est.2022.104124.

36. Tang, H.; Zhang, W.; Fan, C.; Xue, S. Parameter Estimation Using a CLPSO Strategy. In Proceedings of the 2008 IEEE Congress on Evolutionary Computation (IEEE World Congress on Computational Intelligence); June 2008; pp. 70–74.

37. Tang, H.; Xie, L.; Xue, S. Usage of Comprehensive Learning Particle Swarm Optimization for Parameter Identification of Structural System: *International Journal of Natural Computing Research* **2015**, *5*, 1–15, doi:10.4018/ijncr.2015040101.

38. Yousri, D.; Fathy, A.; Babu, T.S.; Berber, M.R. Estimating the Optimal Parameters of Solid Oxide Fuel Cell-based Circuit Using PARASITISM-PREDATION Algorithm. *Intl J of Energy Research* **2021**, *45*, 18018–18032, doi:10.1002/er.6946.

39. Zhuang, S.; Gao, Y.; Chen, A.; Ma, T.; Cai, Y.; Liu, M.; Ke, Y. Research on Estimation of State of Charge of Li-Ion Battery Based on Cubature Kalman Filter. *J. Electrochem. Soc.* **2022**, *169*, 100521, doi:10.1149/1945-7111/ac95cf.

40. Salazar, D.; Garcia, M. Estimation and Comparison of SOC in Batteries Used in Electromobility Using the Thevenin Model and Coulomb Ampere Counting. *Energies* **2022**, *15*, 7204, doi:10.3390/en15197204.

41. Yu, X.; Wei, J.; Dong, G.; Chen, Z.; Zhang, C. State-of-Charge Estimation Approach of Lithium-Ion Batteries Using an Improved Extended Kalman Filter. *Energy Procedia* **2019**, *158*, 5097–5102, doi:10.1016/j.egypro.2019.01.691.

42. Álvarez Antón, J.C.; García Nieto, P.J.; García Gonzalo, E.; Viera Pérez, J.C.; González Vega, M.; Blanco Viejo, C. A New Predictive Model for the State-of-Charge of a High-Power Lithium-Ion Cell Based on a PSO-Optimized Multivariate Adaptive Regression Spline Approach. *IEEE Transactions on Vehicular Technology* **2016**, *65*, 4197–4208, doi:10.1109/TVT.2015.2504933.

43. Liang, J.J.; Qin, A.K.; Suganthan, P.N.; Baskar, S. Comprehensive Learning Particle Swarm Optimizer for Global Optimization of Multimodal Functions. *IEEE Trans. Evol. Computat.* **2006**, *10*, 281–295, doi:10.1109/TEVC.2005.857610.

44. Zhang, H.; Yang, C.; Qiao, J. Emotional Neural Network Based on Improved CLPSO Algorithm For Time Series Prediction. *Neural Process Lett* **2022**, *54*, 1131–1154, doi:10.1007/s11063-021-10672-x.

45. Xiong, W.; Mo, Y.; Zhang, F. Lithium-Ion Battery Modeling and State of Charge Estimation. *Integr. Ferroelectr.* **2019**, *200*, 59–72, doi:10.1080/10584587.2019.1592620.

46. Liu, Y.; Li, J.; Zhang, G.; Hua, B.; Xiong, N. State of Charge Estimation of Lithium-Ion Batteries Based on Temporal Convolutional Network and Transfer Learning. *IEEE Access* **2021**, *9*, 34177–34187, doi:10.1109/ACCESS.2021.3057371.